AUTHORS:
Monray D. Belelie[1]
Nisa Ayob[1]
Roelof P. Burger[1]
Andrew D. Venter[2]
Stuart J. Piketh[1]

AFFILIATIONS:
[1]Unit for Environmental Sciences and Management, North-West University, Potchefstroom, South Africa
[2]Sasol, Secunda, South Africa

CORRESPONDENCE TO:
Monray Belelie

EMAIL:
Monray.Belelie@nwu.ac.za

DATES:
Received: 15 Oct. 2023
Revised: 04 Nov. 2024
Accepted: 14 Nov. 2024
Published: 27 Mar. 2025

HOW TO CITE:
Belelie MD, Ayob N, Burger RP, Venter AD, Piketh SJ. Atmospheric mercury dispersion over the South African Highveld. S Afr J Sci. 2025;121(3/4), Art. #17029. https://doi.org/10.17159/sajs.2025/17029

ARTICLE INCLUDES:
☒ Peer review
☐ Supplementary material

DATA AVAILABILITY:
☐ Open data set
☐ All data included
☒ On request from author(s)
☐ Not available
☐ Not applicable

EDITORS:
Jennifer Fitchett
Pfananani Ramulifho

KEYWORDS:
coal-fired power plants, mercury, South African Highveld, CALPUFF, deposition

FUNDING:
None

Atmospheric mercury dispersion over the South African Highveld

Coal combustion in coal-fired power plants is the dominant source of mercury (Hg) emissions in South Africa. The majority of these plants are located in the South African Highveld, an area that experiences poor air quality. Despite this, the specifics of Hg emissions – such as the amounts emitted, mercury species emitted and their spatial variability – from these plants remain unclear. This study presents the first dispersion modelling of Hg concentrations and wet and dry deposition in the Highveld using CALPUFF. It focuses on inorganic gaseous elemental (Hg^0), inorganic reactive gaseous (Hg^{2+}) and inorganic particle-bound Hg (HgP) emissions from 12 coal-fired power plants from 2011 to 2014. Results show that Hg concentrations are highest near the central cluster of power plants, with levels ranging from 0.0028 to 0.0631 ng/m^3 for Hg^0, 0.0028 to 0.0497 ng/m^3 for Hg^{2+} and 0.0008 to 0.0137 ng/m^3 for HgP. Significant wet and dry deposition, measured at 0.07–7.46 and 0.03–3.33 (g/ha)/year, respectively, also occurs in these areas, indicating that proximity to power plants leads to higher deposition. A health risk assessment suggests that nearby populations may be at risk of acute health impacts from Hg^0 inhalation. However, the accuracy of this assessment is limited by the overestimation of Hg^0 concentrations in dry deposition modelling. The findings highlight the need for further studies to characterise and quantify methylmercury, the most toxic form of Hg, in the environment. This study also potentially shows important locations where new Hg monitoring stations should be placed.

Significance:

The research presents the results of the first-ever dispersion modelling study regarding mercury concentrations and wet and dry deposition over this region using CALPUFF. The findings significantly contribute to scientific knowledge on the spatial variation and deposition of Hg in this region. The study conducts a brief health risk assessment, suggesting that the population working and living near power plants may be at risk of acute adverse health impacts due to inhalation of Hg^0. The findings indicate that further studies are needed to characterise and quantify methylmercury concentrations, as this is mercury's most toxic environmental form, and point to important future research directions.

Introduction

The industrialised South African Highveld Area has been identified as an area associated with poor air quality due to high emissions of criteria pollutants such as particulate matter (PM), SO_2 and NO_x, and a potential area of high concentration of atmospheric mercury (Hg) species.[1] This region is well-known for its various anthropogenic emission sources: coal-fired power plants, coal ash disposal sites, metallurgical smelters and mines, agriculture, transportation and domestic fuel combustion.[2,3]

Globally and annually, combustion in coal-fired power plants is the dominant anthropogenic source of environmental Hg[4], contributing approximately 56%[5]. Coal-fired power plants were estimated as the leading possible anthropogenic source of ambient Hg emissions in South Africa, contributing 72–78% to atmospheric emissions during 2006.[1] The concentration of Hg emitted by the power plants is mainly dependent on the type of emission control device installed. The emission control devices South African power plants use are electrostatic precipitators, fabric filters, desulfurisation/flue-gas conditioning, or a combination thereof.[6] These devices reduce the amounts of particulate matter and sulfur, as well as Hg, with the power plants fitted with fabric filters reducing the highest Hg per GWh.[7,8]

Moreover, a past study listed South Africa as the second-highest global atmospheric Hg emissions source. According to their study, the country contributed about 16% of global Hg emissions.[5] However, these estimates were based on incorrect Hg-content coal values and triggered subsequent Hg studies. Using correct values, the Hg inventory was updated, and South Africa was listed as the sixth leading emitter of the pollutant.[3]

Mercury is a highly toxic and ubiquitous volatile metal, which is environmentally persistent and prone to long-range atmospheric transport.[9] It subsequently leads to adverse health effects in distant regions far from where it was emitted.[10] Mercury is, therefore, regarded as a global pollutant, threatening both the health of humans and ecosystems.[9-12] It is known that the ecological behaviour of the Hg emitted depends on the different environmental forms, as these chemical forms have other chemical properties.[11,12]

Unlike other heavy metals in the environment, atmospheric Hg generally occurs in its gaseous phase.[13] It may be emitted into the atmosphere as inorganic gaseous elemental (Hg^0), inorganic reactive gaseous (Hg^{2+}) and inorganic particle-bound Hg (HgP).[14,15] Atmospheric emissions of Hg are dominated by Hg^0 (53%), followed by Hg^{2+} (37%) and HgP (10%).[16] Although Hg^0 is the predominant form in the gaseous phase[16,17], Hg^{2+} significantly influences the total deposition of atmospheric Hg as it is more reactive and soluble[18]. Under certain conditions, Hg^0 may be removed by dry deposition processes.[19] Mercury is transported over long distances in the atmosphere, even reaching the poles.[10] Due to the concentration of significant sources over the Highveld, it is expected that Hg is transported and deposited over large portions of South Africa.[2] However, there are not many measurements to support this, except for some over the Highveld[20,21] and at background sites (e.g. Bredenkamp[22]).

To investigate and better understand the environmental fate and behaviour of Hg, and given the complex nature of air quality evaluation, air quality models have been developed and established.

In South Africa, the atmospheric dispersion of Hg has been simulated at Cape Point using GEOS-Chem[23,24], GLEMOS, ECHMERIT[24] and the CAM-Chem[25] models. No literature has been found to describe air pollution dispersion modelling of Hg on the industrialised Highveld or with CALPUFF for South Africa. This research aims to fill this knowledge gap and build upon the region's recent and first-ever Hg concentration characterisation study.[20] A health risk assessment was also conducted based on the results obtained from the model for Hg species concentrations.

Material and methods

Understanding the difficulties related to source-specific air pollution control and air quality management can be quite challenging because a wide range of contaminants are emitted from various sources over different spatial and temporal scales. Therefore, specialists in controlling and managing air pollution rely on these models to aid them in decision-making processes for different pollution control settings. Rather than comparing an air pollution source's compliance to results obtained from air pollution sampling, they are based on emission estimates from atmospheric dispersion models.[26]

These models use different tools and strategies, such as Lagrangian, Eulerian, Computational Fluid Dynamics and Gaussian models.[27] It was decided that the Lagrangian California Puff (CALPUFF) modelling system is the best for this study based on its pros and cons and regulatory approval by the South African government.[28] The US EPA also endorses the model for complex topographies and for modelling the atmospheric dispersion of pollutants prone to long-range transport.[29] This recognition was a significant consideration, especially given the intricate topography of the Highveld region and the large size of the domain being studied in the present study. The model has been used to approximate population exposure from power-generating plant emissions to $PM_{2.5}$, SO_2, SO_4, NOx, NO_3 and HNO_3 in Beijing, China[30]; an exposure assessment to Zn, Pb and Cd from a Zinc smelter in Spelter, West Virginia[31]; and for a health risk assessment to Hg emissions from a solid waste gasification plant located southeast of Milan, Italy[32].

Modelling structure and domain

A 250 km by 250 km modelling domain spanning the South African Highveld Area was selected for this study (Figure 1). The Lambert Conic Conformal projection minimises map distortion over this domain size. The components of the CALPUFF modelling system (version 6.42) sequentially consist of CALMET, CALPUFF and CALPOST. In addition, CALSUM was used, which allows the user to combine multiple outputs from CALPUFF into a single file to lessen the runtime considerably.

The modelling domain hosts various anthropogenic sources of Hg, including the 12 power plants illustrated in Figure 1. The power plants, arranged alphabetically, are labelled from 'a to l'. Other possible sources of Hg that were not modelled are combustion in gasification plants, ferrous and non-ferrous metal production, domestic burning, crude oil refining, cement production, waste deposition and incineration, and illegal artisanal gold mining.

CALMET

CALMET meteorological model generates hourly temperature and wind files for the selected domain on a three-dimensional grid.[30] In addition, two-dimensional surface and dispersion characteristics, properties and atmospheric mixing height files are created.[33] For this study, CALMET was run in a hybrid mode from January 2011 to December 2013 at a resolution of 1 km by 1 km using fifth-generation prognostic Mesoscale Model (MM5) data. The MM5 model had a grid resolution of 12 km by 12 km, incorporating Dudhia's simple-ice microphysics, the medium-range forecast Planetary Boundary Layer scheme and a multilayer soil model. The MM5 model was set up using the NCEP Global Reanalysis data, featuring a global grid resolution of 2.5 by 2.5 degrees. The MM5 data set comprises precipitation, wind speeds and vectors, boundary layer heights and temperatures. Pretorius et al.[34] used the same domain and meteorological fields from CALMET to evaluate health risk exposure to PM, SO_4 and NO_3. Pretorius et al.[34] assessed the performance of CALMET for the Highveld region and found the created fields adequately simulated the actual fields. The default CALMET options were mainly used, but some were altered to suit the needs of this study. These alterations and their motivations are summarised in Table 1 and were based on a peer-reviewed report.[35] South Africa does not have the MM5 data set commercially available yet, and it was purchased from

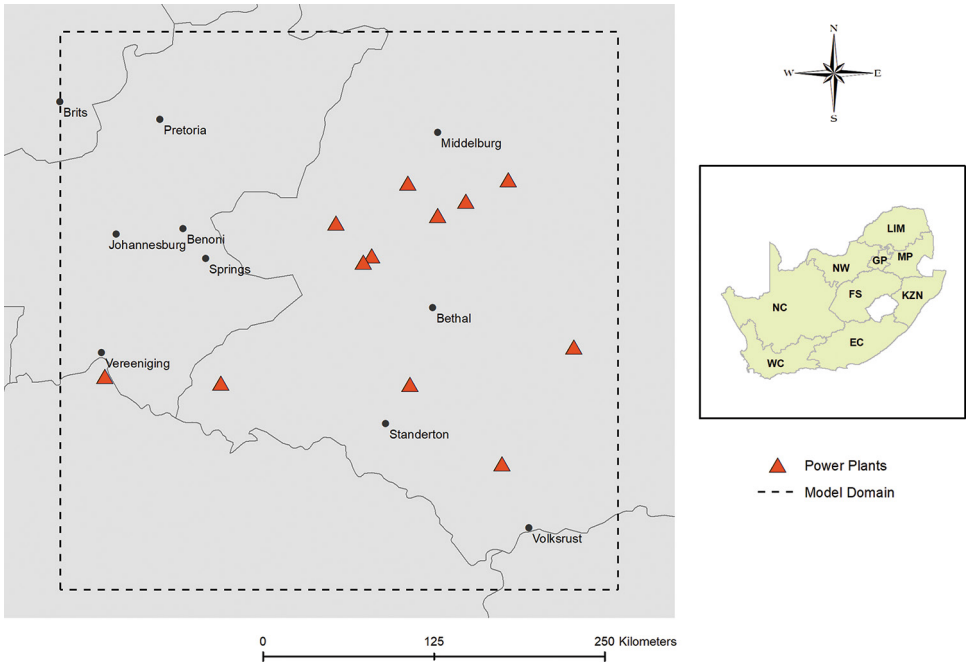

Figure 1: Locations of the 12 coal-fired power plants used to model the atmospheric dispersion of Hg^0, Hg^{2+} and HgP in this study. The black box represents the modelling domain.

Table 1: CALMET options that were altered from the default settings[35]

Description	Default setting	Used setting	Motivation
Map projection	UTM	LCC	To keep map distortion to a minimum
No observation mode	Observations only	No surface, overwater or upper air observation. Use of MM5 data for these observations	Limited observational data
Extrapolation of surface wind	Ignore upper air station data	No extrapolation	Exclusion of observations
Gridded prognostic wind field	No	Yes	Exclusion of observations
3D Relative humidity	Use observations	Use prognostic data	Exclusion of observations
3D temperature	Use observations	Use prognostic data	Exclusion of observations

Table 2: Per annum emission rate of Hg^0, Hg^{2+} and HgP during 2011–2013, in grams per second (g/s) investigated in this study, and the emission control device/s installed at each power-generating plant

Power plant	Emission control device	Emission rate per annum (g/s)			Power plant figure label
		Hg^0	Hg^{2+}	HgP	
ARNOT	FF	0.00212	0.00148	0.0004	a
CAMDEN	FF	0.00318	0.00222	0.0006	b
DUVHA	ESP+FF	0.01431	0.00999	0.0027	c
GROOTVLEI	ESP+FF	0.00848	0.00592	0.0016	d
HENDRINA	FF	0.00212	0.00148	0.0004	e
KENDAL	ESP	0.05406	0.03774	0.0102	f
KOMATI	ESP	0.00954	0.00666	0.0018	g
KRIEL	ESP	0.02915	0.02035	0.0055	h
LETHABO	ESP	0.0636	0.0444	0.0102	i
MAJUBA	FF	0.00689	0.00481	0.0013	j
MATLA	ESP	0.03233	0.02257	0.0061	k
TUTUKA	ESP	0.03339	0.02331	0.0063	l

Lakes Environmental Software, Canada. At a resolution of 12 km along with 18 vertical heights, it was the best accessible data set, with its centre at 26.47 S 29.03 E.

CALPUFF

CALPUFF does not have a dedicated chemical scheme to handle the conversion and transformation of Hg in the atmosphere. A recent study addressed this absence by modifying version 7 of the software to simulate Hg in flue gases and airsheds.[36] However, the present study used the default HNO_3 scheme of the model for reasons discussed hereafter.

The model was used to simulate the hourly concentrations of the three critical atmospheric species of Hg (Hg^0, Hg^{2+} and HgP) and concurrent wet and dry deposition over the domain. The emission rates of Hg utilised in this study were calculated using emission rates for each power-generating plant, obtained directly from ESKOM based on their 2014 Hg emission calculations from each power plant stack (Table 2). The Hg speciation was assumed to be consistent with values reported by Carpi[16], namely Hg^0 (53%), Hg^{2+} (37%), and HgP (10%). Source-specific characteristics of the 12 power-generating plants are summarised in Table 3. The chemical and deposition parameters required for the wet and dry deposition simulation were obtained from Xu et al.[36] and McGuire et al.[37] and are summarised in Table 4.

Generally, the Hg^{2+} and HgP species are dispersed locally, and their deposition patterns depend on local sources.[38] In this study, similar to a previous one, the deposition parameters for Hg^{2+} are assumed to be like those of nitric acid (HNO_3) provided in the model[33], as they provide a conservative basis of deposition for this species[37]. This assumption is conservative as one cannot be sure that the deposition prediction is 'correct'. Here, conservative means that the selected parameters, as detailed below, lead to higher deposition. Hg^{2+} and HNO_3 have similar[36] but not precisely the same aqueous solubility. The modelling parameters for Hg^{2+} are usually assumed to be similar to those of HNO_3 in many settings[39], as both these species are highly soluble and reactive[39,40]. From the limited measurements made regarding the deposition of Hg^{2+}, it may be derived that its deposition velocity magnitude is analogous to HNO_3.[39] The parameters for HgP were adopted from those given for NO_3 in the model.[33,39] This assumption was made to provide a conservative basis for the deposition of this species, and it was decided to make the same assumption. Theoretically, this assumption seems plausible because HgP mainly consists of particles smaller than 2.5 μg/m³.[40,41]

According to [42] and [43] to further justify this assumption, NO_3 is one of the dominant constituents of the fine PM fraction. Deposition velocities of particulate species mainly depend on their size distribution.[39] Therefore, a mass mean diameter of 0.48 μm was selected as particulates resulting from combustion sources are generally less than one micron[37],

Table 3: Source-specific parameters of each power-generating plant investigated in this study

Power plant	Coordinates		Output capacity (MW)	Stack height (m)	Effective stack diameter (m)	Exit velocity (m/s)	Exit temperature (K)
	x (Easting)	y (Northing)					
ARNOT	–25.944	29.792	2100	195	16	25	418
CAMDEN	–26.62	30.091	1600	155	17	14	423
DUVHA	–25.961	29.339	3600	300	18	27	413
GROOTVLEI	–26.77	28.5	1200	152	13	22	418
HENDRINA	–26.031	29.601	2000	155	16	22	418
KENDAL	–26.088	28.969	4100	275	19	24	413
KOMATI	–26.091	29.422	1000	220	17	10	418
KRIEL	–26.254	29.18	3000	213	20	19	413
LETHABO	–26.740	27.975	3700	275	17	28	433
MAJUBA	–27.28	29.771	4100	250	17	35	398
MATLA	–26.28	29.142	3500	275	19	26	408
TUTUKA	–26.776	29.352	3600	275	17	19	413

Table 4: Deposition and chemical parameters of the three species modelled in this study[33,36,37]

Dry deposition (gases)					
Species	**Diffusivity (cm^2/s)**	**Alpha Star**	**Reactivity**	**Meso resistance**	**Henry's Law coefficient**
Hg^0	0.1628	1	18	0	1.00E-07
Hg^{2+}	0.1628	1	18	0	1.00E-07

Dry deposition (particles)		
Species	**Geometric mass mean diameter (microns)**	**Geometric standard deviation (microns)**
HgP	0.48	2

Wet deposition		
Species	**Scavenging coefficient (liquid) s^{-1}**	**Scavenging coefficient (frozen) s^{-1}**
Hg^{2+}	6.00E-05	0
HgP	0.0001	3.00E-05

providing an additional conservative basis for this study. An earlier study used similar deposition parameters for this species, assuming the same geometric mass mean diameter.[44] To make deposition modelling of HgP more reliable[39], suggests that prospective studies regarding the size of these particles should be improved. The deposition parameters for Hg^{2+} and HgP were selected because they imply that the highest possible amount of these deposition-prone species can be removed from the atmosphere, which will have a subsequent and indefinite impact on the modelled Hg concentration. This supposition is not made for Hg^0 as[11] describes wet deposition processes as being inefficient in the removal thereof. For its dry deposition, however, it was modelled to have dry deposition parameters identical to those of Hg^{2+}. A subsequent study by Xu et al.[36] indicated that the dry deposition of Hg^0 should be modelled using a diffusivity value of 0.1194 cm^2/s—lower than the 0.1628 cm^2/s applied in this study. The reactivity value was also supposed to be 8 and not 18. Additionally, the study suggested that the diffusivity for Hg^{2+} should be aligned with that of mercury chloride ($HgCl_2$), which is 0.086 cm^2/s, rather than the 0.1628 cm^2/s previously used. In other words, the dry deposition values reported here are conservative in that the assumed parameters will greatly overestimate the dry deposition of Hg^0 and may underestimate the ambient concentrations underpredicted.

After each run, the 36 output files (12 each for concentration, wet deposition and dry deposition) were merged using CALSUM. This merging was feasible because the modelling periods were consistent, and the species were identical and in the same sequence across runs. Subsequently, CALPOST processed these files to determine the combined concentrations and total wet and dry deposition.

Assessment of potential health risk

As described previously, exposure to Hg could cause adverse impacts on human health. To put the model results into perspective, the potential impact of the simulated emissions from the power plants on health is assessed. A previous study in this region assessed human health

exposure to PM, SO_2 and NO_x emissions from power plants based on intake and intake fraction.[34] The methodology used in this assessment is discussed in detail in previous publications.[45-47] Examples of the method application include evaluating the health risk to Hg from a Malaysian coal-fired power plant[48] and, more recently, exposure to total gaseous mercury from industrially influenced Polish sites[49]. It essentially entails executing four steps, which are discussed in the following sections.

Hazard identification

Hazard identification is an exercise to determine whether the exposure to the pollutant under investigation can cause an intensification in the occurrence of a specific severe health effect in humans. Mercury, a non-carcinogenic pollutant[50], may cause neurological and behavioural conditions in humans[51]. These conditions can be acute, chronic and even fatal[52], and their severity depends on the level of exposure[51]. The primary exposure pathway for Hg^0 is inhalation, particularly in occupational settings where Hg-vapour is present. However, exposure to Hg^0 compounds through ambient air is minimal for the general population.

In contrast, exposure to organic methylmercury primarily occurs via ingestion from dietary sources such as seafood, fish and sea mammals.[52] Reactive and particulate Hg are commonly removed near their sources due to their high atmospheric solubility and reactivity.[53,54] They risk human health after deposition, when methylmercury, the most toxic form of Hg, may be formed.[55,56] This study, however, only considers the inhalation exposure pathway to Hg^0.

Dose response

Fundamentally, this step of the risk assessment process establishes an exposure-response relationship. The toxicological factors demonstrating this relationship are Reference Concentration (RFC) and Reference Dose (RFD). The RFC evaluates inhalation risks, while the RFD assesses the risks associated with oral exposure. Both reference doses are benchmarks of daily human exposure[45,50], defining them as average daily exposure levels that are not likely to threaten human health throughout a lifetime. Typically, this step requires the implementation of an equation to calculate an RFD value, which can be adjusted to calculate RFC. However, this practice is not recommended in studies investigating inorganic compounds[57] because they differ fundamentally from organic compounds containing carbon-hydrogen bonds. As an RFC value was readily available, this study deviates from the standard procedure. The RFC value used in this risk assessment, associated with Hg^0 inhalation, is adopted from IRIS[50] (0.3 $\mu g/m^3$). This value is used to characterise the risk exposure to Hg^0 in the fourth step of this process. It is also assumed to be identical for acute and chronic exposure periods.[50]

Assessment of exposure

The exposure of the human population to Hg^0 was predicted, where the highest cumulative concentration of Hg^0 was simulated during the three years using CALPUFF as described in the CALPUFF section previously. The simulation returned modelled hourly, 8-hourly and periodic (cumulative annual) Hg^0 concentrations. These values assessed potential acute and chronic impacts on human health. Notably, the chosen exposure continuity – reflecting typical working hours – allows for a comprehensive evaluation of health risks associated with ambient air concentrations.[58]

Two scenarios were considered: a baseline scenario that evaluated the minimum Hg^0 concentrations, and a worst-case scenario that assessed the maximum concentrations for both acute and chronic exposure.

Characterisation of risk

The US EPA[57] recommends Risk Exposure Levels (REL)[59] as the preferred choice to assess acute inhalation values. Like an RFC, a REL is the air concentration at or beneath which no severe health impacts are expected in the population over a given exposure period. The population includes susceptible subgroups such as children, senior citizens and maternal exposure.[57] In our analysis, we utilised the RFC value for assessing chronic exposure, while the US EPA-recommended REL values were employed for acute exposure scenarios. While RFC and REL serve distinct purposes, they were used interchangeably in the formula below for comparative purposes. The cumulative hourly, 8-hourly and annual Hg^0 concentrations are compared to acute (1 hourly and 8-hourly) and chronic REL values to assess potential health impact. Additional information, including associated uncertainty factors, is provided in Table 5.

For the characterisation of a health risk for a non-carcinogenic pollutant by way of inhalation, the hazard must be quantified through the use of the hazard quotient (HQ)[57] given by Equation 1:

$$HQ = EC/RFC \qquad \text{Equation 1}$$

where EC represents the exposure concentration in the air ($\mu g/m^3$), and RFC is the reference concentration ($\mu g/m^3$). If HQ is smaller than 1, it indicates that the pollutant concentration is less than the RFC benchmark value. If this is the case, no subsequent action is necessary because the likely risk is within the permissible threshold. In other words, it means that $HQ < 1$ is considered safe. It does not mean that $HQ > 1$ should be construed as causing potential severe health impacts. It should instead be deduced as an indication of potential severe health impacts.[60]

Results and discussion

Atmospheric dispersion of Hg species

The modelled spatial distribution of Hg^0, Hg^{2+} and HgP concentrations is illustrated in Figure 2. The highest cumulative ambient concentrations of all three Hg species were calculated over the central parts of the modelled domain (0.0497–0.0631 ng/m^3 for Hg^0 and Hg^{2+} and 0.0123–0.0137 ng/m^3). As expected, this is the same spatial distribution as the other primary pollutants from power plants modelled for the Highveld region.[34] Moreover, as expected, the highest modelled concentrations were observed for Hg^0 and the lowest for HgP. The modelled concentrations for Hg^0, Hg^{2+} and HgP ranged from 0.0028 to 0.0631 ng/m^3, 0.0028 to 0.0497 ng/m^3 and 0.0008 to 0.0137 ng/m^3, respectively. These results are comparatively lower than the ambient monitored total gaseous mercury concentrations (comprising Hg^0 and Hg^{2+}) at three study domain sites (Balfour, Middelburg and Standerton).[20] During a one-year monitoring period in 2009, average concentrations at the sites were measured at 1.99 ± 0.94 ng/m^3, 1.04 ± 0.62 ng/m^3 and 1.25 ± 1.38 ng/m^3, respectively. In comparison to the USA[61], reported ambient total gaseous Hg (Hg^0+Hg^{2+}) concentrations near a coal-fired power plant (<1 km) ranged from 1.5 ± 0.2 ng/m^3 to 1.7 ± 0.3 ng/m^3. Additionally, studies in Australia indicate average Hg_0 concentrations of 0.90 ± 0.10 ng/m^3,[62]

Table 5: Uncertainty associated with REL values (OEHHA, 2014)[59] used for comparison

RFC comparison	REL ($\mu g/m^3$)	Species	Study population	Exposure continuity	Exposure duration	Composite uncertainty factor
Acute (1 hour)	0.6	Rats	12	–	1 hour per day	3000
Acute (8 hours)	0.06	Humans	236	8 hours per day, five days a week	13.7–15.6 years	3000
Chronic	0.03	Humans	236	8 hours per day, five days a week	13.7–15.6 years	300

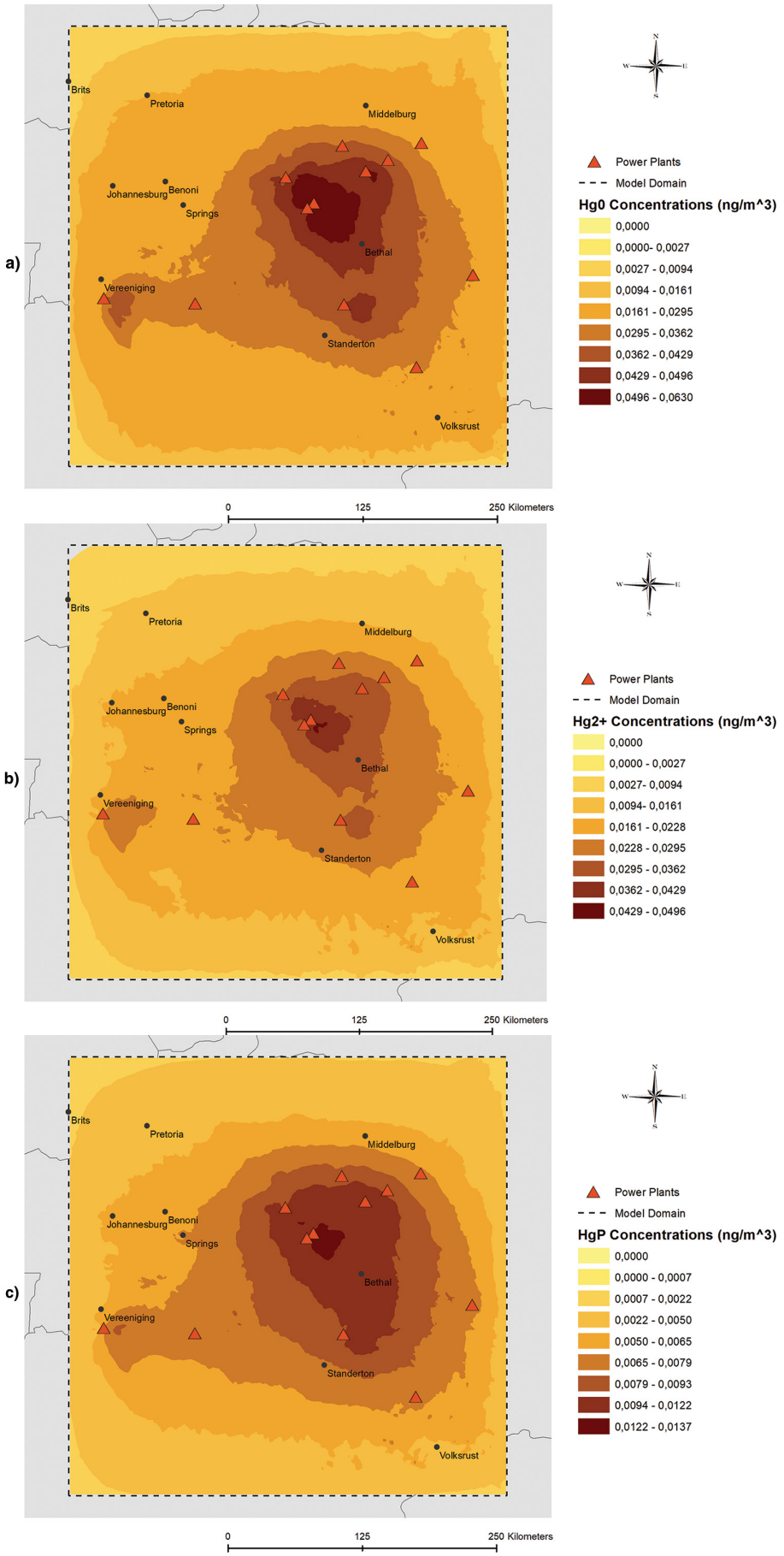

Figure 2: The spatial distribution of three-year (2011–2013) modelled average (a) Hg^0, (b) Hg^2+ and (c) HgP concentrations (ng/m^3), originating from power plants on the South African Highveld.

while total gaseous Hg concentrations in eastern China were significantly higher, at 4.91 ± 3.66 ng/m^3.[63]

The monitoring sites, depicted in Figure 1, were influenced by different Hg emission sources, from local fossil fuel combustion to sparse regional contributions. A notable finding from the study was that domestic burning constituted the most significant source of emissions throughout the monitoring period. Domestic burning is a low-level source with emissions likely to be confined beneath the boundary layer, so this source should be factored into future Hg modelling efforts. The proximity of Kriel and Matla power plants, which may act as a single emission source due to their closeness, contributes to an accumulation of polluted air in an area already burdened with high Hg concentrations. Their proximity and lower emission heights and dispersion potential could lead to localised increases in Hg levels. Nevertheless, it is crucial to acknowledge that the peak concentrations are influenced by specific source characteristics and local atmospheric conditions rather than the mere expansion of the modelling domain.

The size of the modelling domain can influence the extent to which deposition processes remove Hg species. This influence on removal potential is particularly true for Hg^0, which, due to its solubility and reactivity, has a longer atmospheric lifetime and, thus, a greater potential for deposition over a larger area. However, it is essential to recognise that the concentration gradients of Hg species, including Hg^0, are primarily governed by their emission rates, atmospheric chemistry and local meteorological conditions. These factors collectively determine the dispersion and deposition patterns observed in our model.

Wet and dry deposition

The modelled spatial wet distribution of Hg^{2+} and HgP concentrations is illustrated in Figure 3. The wet deposition of Hg^0, due to reasons

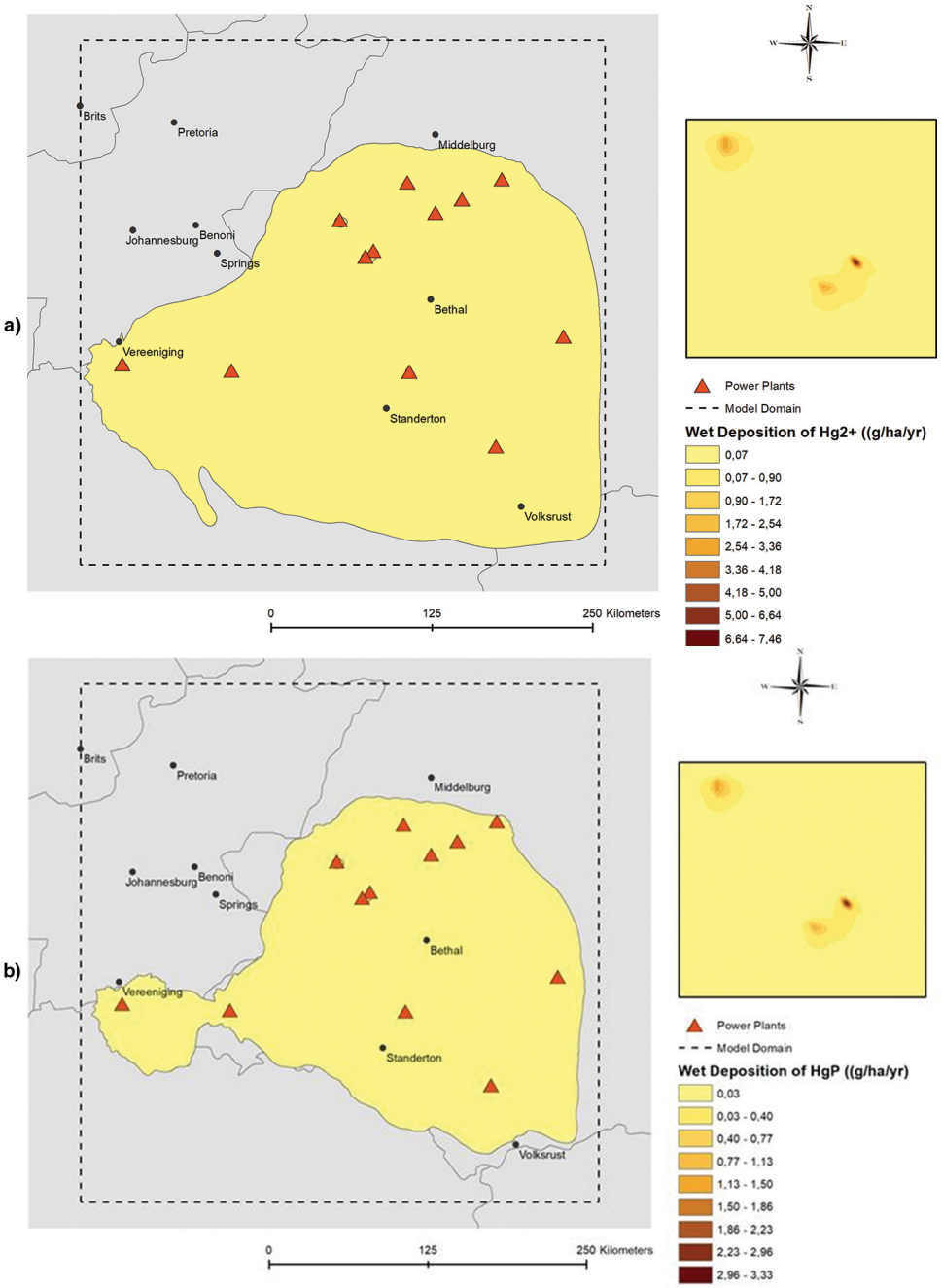

Figure 3: The spatial distribution of averaged three-year modelled wet deposition (g/ha)/year) of (a) Hg^{2+} and (b) HgP on the South African Highveld. The reference box to the right shows a zoomed-in view of the modelled deposition over Kriel and Matla.

discussed previously, is ignored. The results reveal that relatively low amounts of each species were removed from most of the modelled region. However, over four locations on the domain, higher amounts were removed in the locations' immediate vicinity (<1km) – not visible on the maps unless zoomed in to a power plant. The previous was simulated in the atmosphere surrounding Kriel, Matla, Lethabo, Kendal and Tutuka. This observation may be explained by the fact that species of Hg tend to be deposited near their emission source.[16,64] The simulated wet deposition of Hg^{2+} and HgP during the modelling period ranged from 0.07 to 7.46 and 0.03 to 3.33 (g/ha)/year, respectively. Notably, the present study's wet deposition values are significantly higher than those measured in suburban, agricultural and traffic areas in China (0.001–0.007 (g/ha)/year).[65] This disparity can be attributed to the fact that the current study focused on modelled rather than measured wet deposition. Additionally, the differences may stem from the assumed modelling parameters used in this study.

The modelled spatial dry distribution of Hg^{2+} and HgP concentrations is illustrated in Figure 4. Notably, the dry deposition of Hg^0 was interpreted cautiously, as its dry deposition parameters were assumed to be identical to those adopted for Hg^{2+}, which provides conservative estimates of this species' highest potential dry deposition. Dry deposition is another mechanism by which species of Hg may be transferred from the atmosphere to aquatic and terrestrial surfaces. This mechanism, of course, occurs in the absence of precipitation. The modelled dry deposition of Hg^0 and Hg^{2+} closely resembles one another, with the central parts of the domain being the region most affected, followed by the southwestern part. Dry deposition rates decrease from the centre of the domain to the outskirts. The dry deposition of Hg^0, Hg^{2+} and HgP ranged from 0.003 to 0.104, 0.002 to 0.081, and 0.00002 to 0.00052 (g/ha)/year, respectively. Comparatively, the annual Hg^{2+} dry deposition levels observed in the Four Corners area ranged from 0.022 g/ha/year at the Molas Pass high-elevation remote mountain site to 0.115 g/ha/year at the Mesa Verde National Park site, suggesting that our modelled values are generally lower than those found in the USA.[66] The maximum modelled deposition of Hg^0 (1.4 (g/ha)/year) was simulated to occur mainly over Kriel town (also known as Ga-Nala) (–26.1131; 29.0834) and its immediate vicinity (including Thubelihle settlement). The dry deposition of Hg^{2+} was somewhat different, occurring predominantly near Kriel (–26.1241; 29.0174) and Matla (–26.0731; 29.0700) power plants. On the other hand, the highest dry deposition of HgP was simulated on the outskirts of the domain, increasing from the centre of the domain.

While Hg^0 and Hg^{2+} share similar diffusivity and reactivity (due to the similarity assumption made in the present study), leading to comparable dry deposition rates, HgP's distinct physical properties, such as its geometric mean diameter and standard deviation, result in different deposition behaviour. This variance in physical characteristics may contribute to the observed disparity in dry deposition rates across the domain.

Assessment of potential health risk

The hazard quotient (HQ) has been calculated for emissions of Hg^0 from surrounding Kriel and Matla as a spatial minimum (baseline scenario) and maximum (worst-case scenario) within the study area (Table 6). These values provide a range of HQ that, at its highest, offers an estimate of health risk to the population within 20–40 km from the two power plants. The calculated acute (1 hour and 8 hours) and chronic HQ values for the baseline scenario indicate a tolerable exposure level to concentrations of Hg^0, with all HQ values being less than one (HQ < 1). This scenario's minimum predicted exposure concentrations are below the recommended REL values.

In contrast, for the worst-case scenario, the acute (1 hour and 8 hours) HQ values exceed one (HQ > 1), indicating a potential for severe health effects due to peak emission events. The maximum predicted exposure levels are also above the REL values for these acute exposure periods. However, the HQ value for chronic exposure remains below one (HQ < 1), suggesting that while short-term risks may be significant, long-term risks are within acceptable limits.

In atmospheric dispersion modelling, particularly for hazardous air pollutants Hg^0, several known uncertainties can influence the accuracy of predicted concentrations. Variability in emission factors is a primary source of uncertainty, as actual emissions can fluctuate due to changes in power plant operations, fuel composition and the effectiveness of emission control technologies. Meteorological data like those from MM5 drive the dispersion patterns in models like CALPUFF and may introduce another layer of uncertainty. Examples include inaccuracies in wind speed, direction, atmospheric stability and other weather-related variables that can significantly alter the model outputs. As shown by de Lange et al.[67], the simulated planetary boundary layer may also have had a large impact on the dispersion as this region does not have information on the vertical structure of the atmosphere. The specified deposition rates, chemical transformation rates and mixing heights are often based on assumptions or limited data, which can lead to either overestimation or underestimation of concentrations. Despite these uncertainties, modelling remains vital for assessing potential health risks from air pollution. However, it is essential to interpret the results within the context of these limitations and the lack of a South African national ambient standard for mercury.

Conclusions

As expected, the concentrations of the Hg species are highest over the cluster of power plants situated in the centre of the domain. Moreover, the results convey that concentrations of the species are accumulating in an area of already high concentrations over Kriel and Matla. The concentrations are already high given the proximity of the power plants and other Hg sources to one another and because power plants are the predominant source of Hg in South Africa. This part of the domain also yielded maximum wet and dry deposition. It is thus clear that the proximity of the power plants leads to higher deposition. Once deposited, inorganic mercury can be converted into methylmercury, a highly toxic form that bioaccumulates in aquatic food chains, by certain microbial processes in water systems. The formation of methylmercury is, therefore, likely to occur due to the possibility of these high-modelled concentrations being removed by deposition. The high wet deposition results for Hg^{2+} cover the same spatial area as the modelled concentration, corroborating the above statement. It could expose the population that depends on fishing to supplement their nutritional needs, such as the Rietspruitdam and Steenkoolspruit rivers near Kriel town. Although conservative estimates, the results identify a potential need to assess the possible impact of toxic methylmercury on the South African Highveld. While acute exposure to peak emissions of Hg^0 from the power plants in the study area may pose severe health risks, chronic exposure remains within acceptable limits. The conservative assumptions used in dry deposition modelling overestimated the expected concentrations of Hg^0 in the ambient air. This discrepancy underscores that this study's health risk assessment is uncertain.

Table 6: Hazard quotient (HQ) assessment of potential health risk to emissions of Hg^0 from modelled power plants

Exposure period	Lowest predicted exposure (μg/m³)	Maximum predicted exposure (ug/m³)	REL (μg/m³)	RFC (μg/m³) used for HQ quantification	Baseline HQ	Worst-case HQ
Acute (1 hour)	0.002	2.001	0.6	0.3	0.007	6.67
Acute (8 hours)	0.001	0.791	0.06	0.3	0.003	2.637
Chronic	0.0000497	0.0000631	0.03	0.3	0.0001657	0.0875

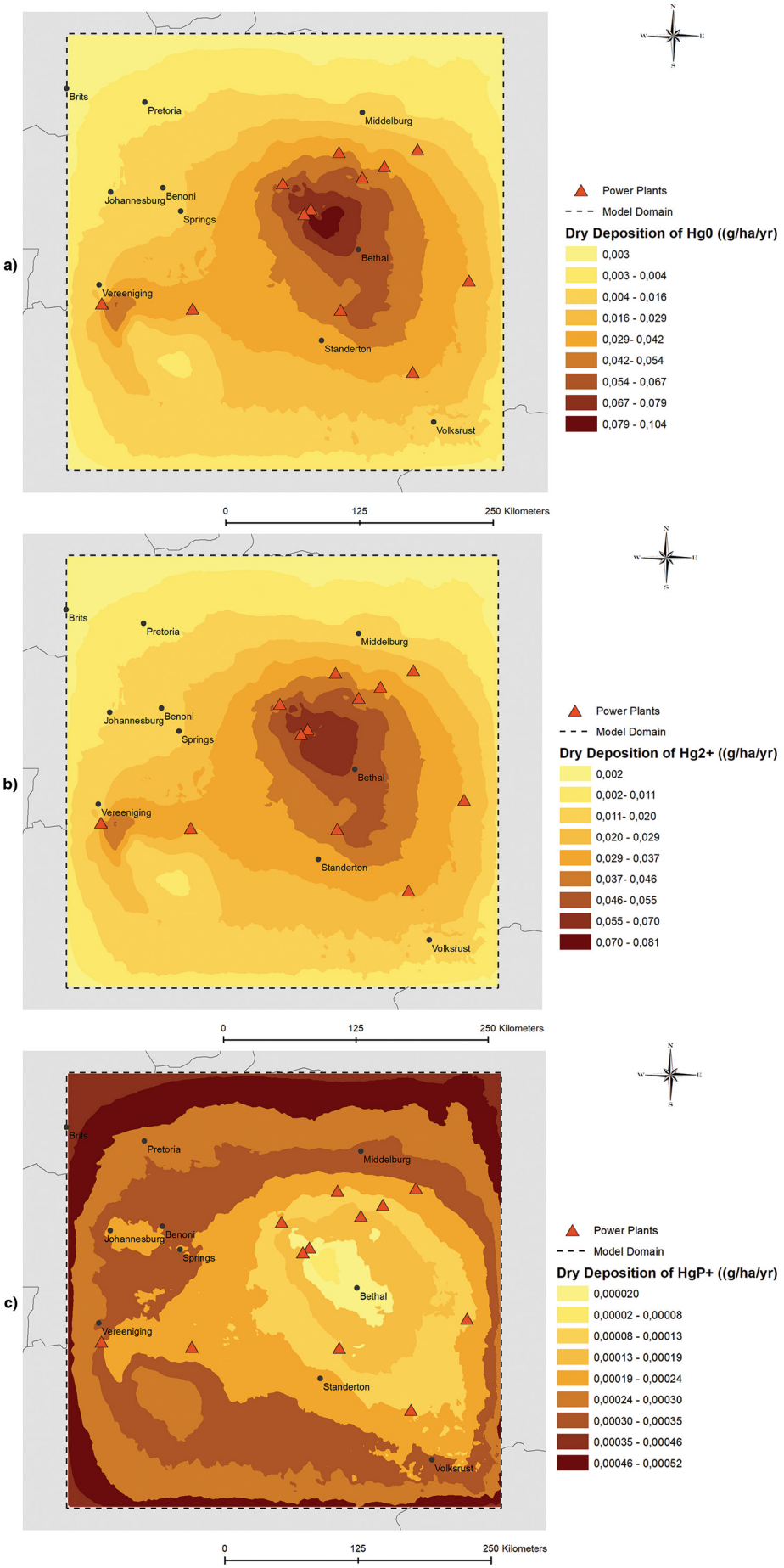

Figure 4: The spatial distribution of averaged three-year modelled dry deposition (g/ha)/year) of (a) Hg^0, (b) Hg^2+ and (c) HgP on the South African Highveld.

Prospective Hg modelling studies and related health risk assessments should improve on this study using the appropriate dry deposition values of Hg^0. The prospective modelling of Hg over this region should include all Hg sources and be evaluated against ambient monitored concentrations during the modelling period to account for uncertainty and fractional bias. The findings suggest potential locations for new Hg monitoring sites. The concurrent use of reanalysis data sets of precipitation may enhance this to provide more refined deposition modelling.

Acknowledgements

We thank ESKOM SOC Ltd for the provision of the power station Hg emission data used in this study.

Data availability

The data supporting the results of this study are available upon request to the corresponding author.

Declarations

This paper emanates from M.D.B.'s MSc dissertation from 2016. We have no competing interests to declare. We have no AI or LLM use to declare.

Authors' contributions

M.D.B.: Data curation, methodology, formal analysis, investigation, writing – original draft. N.A.: Investigation, software, writing – review and editing. R.P.B.: Resources, methodology, supervision, writing – review and editing. A.D.V.: Supervision, writing – review and editing. S.J.P.: Resources, methodology, supervision, writing – review and editing. All authors read and approved the final manuscript.

References

1. Masekoameng KE, Leaner J, Dabrowski J. Trends in anthropogenic mercury emissions estimated for South Africa during 2000–2006. Atmos Environ. 2010;44(25):3007–3014. https://doi.org/10.1016/j.atmosenv.2010.05.006
2. Freiman MT, Piketh SJ. Air transport into and out of the industrial Highveld region of South Africa. J Appl Meteorol. 2003;42(7):994–1002. https://doi.org/10.1175/1520-0450(2003)042<0994:ATIAOO>2.0.CO;2
3. Dabrowski JM, Ashton PJ, Murray K, Leaner JJ, Mason RP. Anthropogenic mercury emissions in South Africa: Coal combustion in power plants. Atmos Environ. 2008;42(27):6620–6626. https://doi.org/10.1016/j.atmosenv.2008.04.032
4. Pacyna EG, Pacyna JM, Pirrone N. European emissions of atmospheric mercury from anthropogenic sources in 1995. Atmos Environ. 2001;35(17):2987–2996. https://doi.org/10.1016/S1352-2310(01)00102-9
5. Pacyna EG, Pacyna JM, Steenhuisen F, Wilson S. Global anthropogenic mercury emission inventory for 2000. Atmos Environ. 2006;40(22):4048–4063. https://doi.org/10.1016/j.atmosenv.2006.03.041
6. Leaner J, Dabrowski J, Mason R, Ashton P, Murray K, Resane T, et al. Mercury emissions from point sources in South Africa. In: Pirrone N, Mason R, editors. Mercury fate and transport in the global atmosphere. New York: Springer; 2009. p. 113–130. https://doi.org/10.1007/978-0-387-93958-2_5
7. Belelie MD, Piketh SJ, Burger RP, Venter AD, Keir JN. Mercury emissions from the power sector in South Africa. In: Annual National Association for Clean Air (NACA) conference; 2016 October 5–7; Mbombela, South Africa. p. 14.
8. Garnham BL, Langerman KE. Mercury emissions from South Africa's coal-fired power stations. Clean Air J. 2016;26(2):14–20. https://doi.org/10.17159/2410-972X/2016/v26n2a8
9. Angot H, Barret M, Magand O, Ramonet M, Dommergue A. A 2-year record of atmospheric mercury species at a background Southern Hemisphere station on Amsterdam Island. Atmos Chem Phys. 2014;14(20):11461–11473. https://doi.org/10.5194/acp-14-11461-2014
10. Pacyna EG, Pacyna JM. Global emissions of mercury from anthropogenic sources in 1995. Water Air Soil Pollut. 2002;137:149–165. https://doi.org/10.1023/A:1015502430561
11. Lindqvist O, Rodhe H. Atmospheric mercury—a review. Tellus B Chem Phys Meteorol. 1985;37B(3):136–159. https://doi.org/10.1111/j.1600-0889.1985.tb00062.x
12. Boudala FS, Folkins I, Beauchamp R, Tordon R, Neima B, Johnson B. Mercury flux measurements over air and water in Kejimkujik National Park, Nova Scotia. Water Air Soil Pollut. 2000;122:183–202. https://doi.org/10.1023/A:1005299411107
13. Ebinghaus R, Jennings SG, Schroeder WH, Berg T, Donaghy T, Guentzel J, et al. International field intercomparison measurements of atmospheric mercury species at Mace Head, Ireland. Atmos Environ. 1999;33(18):3063–3073. https://doi.org/10.1016/S1352-2310(98)00119-8
14. Poissant L, Pilote M, Beauvais C, Constant P, Zhang HH. A year of continuous measurements of three atmospheric mercury species (GEM, RGM, and HgP) in southern Quebec, Canada. Atmos Environ. 2005;39(7):1275–1287. https://doi.org/10.1016/j.atmosenv.2004.11.007
15. Prestbo EM. Wet deposition of mercury in the US and Canada, 1996–2005: Results and analysis of the NADP mercury deposition network (MDN). Atmos Environ. 2009;43(27):4223–4233. https://doi.org/10.1016/j.atmosenv.2009.05.028
16. Carpi A. Mercury from combustion sources: A review of the chemical species emitted and their transport in the atmosphere. Water Air Soil Pollut. 1997;98(34):241–254. https://doi.org/10.1007/BF02047037
17. Lin C-J, Pehkonen SO. The chemistry of atmospheric mercury: A review. Atmos Environ. 1999;33(13):2067–2079. https://doi.org/10.1016/S1352-2310(98)00387-2
18. Ebinghaus R, Kock HH, Schmolke SR. Measurements of atmospheric mercury with high time resolution: Recent applications in environmental research and monitoring. Fresenius J Anal Chem. 2001;371(6):806–815. https://doi.org/10.1007/s002160101048
19. Lindberg SE, Meyers GE, Turner RR, Schroeder WH. Atmospheric-surface exchange of mercury in a forest: Results of modeling and gradient approaches. J Geophys Res. 1992;97(D13):14677. https://doi.org/10.1029/92JD01221
20. Belelie MD, Piketh SJ, Burger RP, Venter AD, Naidoo M. Characterisation of ambient total gaseous mercury concentrations over the South African Highveld. Atmos Pollut Res. 2019;10(1):12–23. https://doi.org/10.1016/j.apr.2018.06.001
21. Meyer R. Ambient mercury concentrations at industrially influenced sites on the Highveld [dissertation]. Potchefstroom: North-West University; 2017.
22. Bredenkamp L. Background ambient atmospheric mercury concentrations for the South African interior [dissertation]. Potchefstroom: North-West University; 2017.
23. Selin NE, Jacob DJ, Park RJ, Yantosca RM, Strode S, Jaeglé L, et al. Chemical cycling and deposition of atmospheric mercury: Global constraints from observations. J Geophys Res. 2007;112(D2), D02308. https://doi.org/10.1029/2006JD007450
24. Travnikov O, Angot H, Artaxo P, Bencardino M, Bieser J, D'Amore F, et al. Multi-model study of mercury dispersion in the atmosphere: Atmospheric processes and model evaluation. Atmos Chem Phys. 2017;17(8):5271–5295. https://doi.org/10.5194/acp-17-5271-2017
25. Lei H, Liang X-Z, Wuebbles DJ, Tao Z. Model analyses of atmospheric mercury: Present air quality and effects of transpacific transport on the United States. Atmos Chem Phys. 2013;13(4):10807–10825. https://doi.org/10.5194/acp-13-10807-2013
26. South African Department of Environmental Affairs (DEA). South African draft regulations regarding air dispersion modelling. Notice 1035 of 2012 in terms of NEM (Act No. 39 of 2004). Pretoria: DEA; 2012.
27. Leelőssy Á, Molnár F, Izsák F, Havasi Á, Lagzi I, Mészáros R. Dispersion modeling of air pollutants in the atmosphere: A review. Cent Eur J Geosci. 2014;6(3):257–278. https://doi.org/10.2478/s13533-012-0188-6
28. South African Department of Environmental Affairs (DEA). South African regulations regarding air dispersion modeling. Notice 163 of 2012 regarding NEM: AQA. No. 39 of 2004. Govt Gaz. 2014 July 11;R533(37804):1–78.
29. US Environmental Protection Agency (EPA). Requirements for preparation, adoption, and submittal of state implementation plans (Guideline on air quality models). Washington DC: US EPA; 2000.

30. Zhou Y, Levy JI, Hammitt JK, Evans JS. Estimating population exposure to power plant emissions using CALPUFF: A case study in Beijing, China. Atmos Environ. 2003;37(6):815–826. https://doi.org/10.1016/S1352-2310(02)00937-8

31. MacIntosh DL, Stewart JH, Myatt TA, Sabato JE, Flowers GC, Brown KW, et al. Use of CALPUFF for exposure assessment in a near-field, complex terrain setting. Atmos Environ. 2010;44(2):262–270. https://doi.org/10.1016/j.atmosenv.2009.09.023

32. Lonati G, Zanoni F. Monte-Carlo human health risk assessment of mercury emissions from a MSW gasification plant. Waste Manag. 2013;33(2):347–355. https://doi.org/10.1016/j.wasman.2012.10.015

33. Scire JS, Strimaitis DG, Yamartino RJ. A user's guide for the CALPUFF dispersion model (Version 5). Concord, MA: Earth Tech, Inc.; 2000.

34. Pretorius I, Piketh S, Burger R. Emissions management and health exposure: Should all power stations be treated equal? Air Qual Atmos Health. 2017;10(4):509–520. https://doi.org/10.1007/s11869-016-0444-x

35. Exponent Inc. Review of the Sasol Atmospheric Impact Report. Maynard, MA: Exponent; 2018. Available from: https://www.srk.com/download/file/2247

36. Xu H, Zhu Y, Wang L, Lin CJ, Jang C, Zhou Q, et al. Source contribution analysis of mercury deposition using an enhanced CALPUFF-Hg in the Central Pearl River Delta, China. Environ Pollut. 2019 July;250:1032–1043. https://doi.org/10.1016/j.envpol.2019.04.008

37. McGuire L, Hoffman VJ, Paulsen S. Report prepared for Western States Petroleum Association, project no. 0032209. Sacramento, CA: WSPA Member Facilities; 2009.

38. Zyśk J, Wyrwa A, Pluta M. Emissions of mercury from the power sector in Poland. Atmos Environ. 2011;45(3):605–610. https://doi.org/10.1016/j.atmosenv.2010.10.041

39. Zhang L, Wright LP, Blanchard P. A review of current knowledge concerning dry deposition of atmospheric mercury. Atmos Environ. 2009;43(37):5853–5864. https://doi.org/10.1016/j.atmosenv.2009.08.019

40. Yarwood G, Lau S, Jia Y. Modelling atmospheric mercury chemistry and deposition with CAMx for a 2002 annual simulation. Final report prepared for Wisconsin Department of Natural Resources. 2003.

41. Dastoor AP, Larocque Y. Global circulation of atmospheric mercury: A modelling study. Atmos Environ. 2004;38(1):147–161. https://doi.org/10.1016/j.atmosenv.2003.08.037

42. Aneja VP, Wang B, Tong DQ, Kimball H, Steger J. Characterization of major chemical components of fine particulate matter in North Carolina. J Air Waste Manag Assoc. 2006;56(8):1099–1017. https://doi.org/10.1080/10473289.2006.10464529

43. Tsai YI, Kuo S. PM2.5 aerosol water content and chemical composition in a metropolitan and a coastal area in southern Taiwan. Atmos Environ. 2005;39(27):4827–4839. https://doi.org/10.1016/j.atmosenv.2005.04.024

44. Sang-Sup L, Keener T. Dispersion modeling of mercury emissions from coal-fired power plants at Coshocton and Manchester, Ohio. Ohio J Sci. 2005;108(4):65–69.

45. Barnes DG, Dourson M. Reference dose (RfD): Description and use in health risk assessments. Regul Toxicol Pharmacol. 1988;8(4):471–486. https://doi.org/10.1016/0273-2300(88)90047-5

46. Louvar J, Louvar B. Health and environmental risk analysis: Fundamentals with applications. Upper Saddle River, NJ: Prentice Hall; 1998.

47. US National Service Center for Environmental Publications (NSCEP). Human health risk assessment protocol for hazardous waste combustion facilities. Washington DC: United States Environmental Protection Agency; 2005.

48. Mokhtar MM, Hassim MH, Taib RM. Health risk assessment of emissions from a coal-fired power plant using AERMOD modeling. Process Saf Environ Prot. 2014;92:476–485. https://doi.org/10.1016/j.psep.2014.05.008

49. Pyta H, Widziewicz-Rzońca K, Slaby K. Inhalation exposure to gaseous and particulate bound mercury present in the ambient air over the polluted area of southern Poland. Int J Environ Res Public Health. 2020;17(14):4999. https://doi.org/10.3390/ijerph17144999

50. IRIS (Integrated Risk Information System). Status of data for mercury, elemental. Washington DC: United States Environmental Protection Agency (US EPA); 1995.

51. World Health Organization (WHO). Guidance for identifying populations at risk from mercury exposure. Geneva: WHO; 2008.

52. United States Department of Health and Human Services. Toxicological profile for mercury. Atlanta, GA: US Department of Health and Human Services; 1999.

53. Landis MS, Stevens RK, Schaedlich F, Prestbo EM. Development and characterisation of an annular denuder methodology for the measurement of divalent inorganic reactive gaseous mercury in ambient air. Environ Sci Technol. 2002;36(13):3000–3009. https://doi.org/10.1021/es015887t

54. Lohman K. Modeling mercury transformation in power plant plumes. Environ Sci Technol. 2006;40:3848–3854. https://doi.org/10.1021/es051556v

55. Hong Y-S, Kim Y-M, Lee K-E. Methylmercury exposure and health effects. J Prev Med Public Health. 2012;45:353–363. https://doi.org/10.3961/jpmph.2012.45.6.353

56. Celo V, Lean DRS, Scott SL. Abiotic methylation of mercury in the aquatic environment. Sci Total Environ. 2006;368(1):126–137. https://doi.org/10.1016/j.scitotenv.2005.09.043

57. US Environmental Protection Agency (EPA). Human health risk assessment protocol for hazardous waste combustion facilities. Washington DC: US EPA; 2005.

58. US Environmental Protection Agency (EPA). Guidelines for human exposure assessment. Washington DC: US EPA; 2019.

59. OEHHA (Office of Environmental Health Hazard Assessment). Appendix D: Individual acute, 8-hour, and chronic reference exposure level summaries. Sacramento, CA; 2014.

60. US Environmental Protection Agency (EPA). Estimated risk: Background on risk characterisation. Washington DC: US EPA; 2013.

61. Gratz LE, Eckley CS, Schwantes SJ, Mattson E. Ambient mercury observations near a coal-fired power plant in a Western U.S. urban area. Atmosphere (Basel). 2019;10(4):176. https://doi.org/10.3390/atmos10040176

62. Fisher JA, Nelson PF. Atmospheric mercury in Australia: Recent findings and future research needs. Elementa: Sci Anthropocene. 2020;8(1):070. https://doi.org/10.1525/elementa.2020.070

63. Nie X, Wang Y, Mao H, Wang T, Li T, Wu Y, et al. Atmospheric mercury in an eastern Chinese metropolis (Jinan). Ecotoxicol Environ Saf. 2020;196, Art. #110541. https://doi.org/10.1016/j.ecoenv.2020.110541

64. Driscoll CT, Han Y-J, Chen CY, Evers DC, Lambert KF, Holsen TM, et al. Mercury contamination in forest and freshwater ecosystems in the northeastern United States. Bioscience. 2007;57(1):17–28. https://doi.org/10.1641/B570106

65. Fang GC, Ni SC, Kao CL, Zhuang YJ, Li KX, Liang GR. Mercury wet depositions study at suburban, agriculture, and traffic sampling sites. Environ Geochem Health. 2021;43:235–245. https://doi.org/10.1007/s10653-020-00695-z

66. Sather ME, Mukerjee S, Smith L, Mathew J, Jackson C, Flournoy MG. Gaseous oxidized mercury dry deposition measurements in the Four Corners area, U.S.A., after large power plant mercury emission reductions. Atmos Pollut Res. 2021;12(1):148–158. https://doi.org/10.1016/j.apr.2020.08.030

67. De Lange A, Naidoo M, Garland RM, Dyson LL. The sensitivity of simulated surface-level pollution concentrations to WRF-ARW-model PBL parameterisation schemes over the Highveld of South Africa. Atmos Res. 2021;254(1), Art. #105517. https://doi.org/10.1016/j.atmosres.2021.105517